

# Enhancement of the photoelectric performance in inverted bulk heterojunction solid solar cell with inorganic nanocrystals



Weiling Luan<sup>a,\*</sup>, Chengxi Zhang<sup>a</sup>, Lingli Luo<sup>a</sup>, Binxia Yuan<sup>a,b</sup>, Lin Jin<sup>a</sup>, Yong-Sang Kim<sup>c</sup>

<sup>a</sup> Key Laboratory of Pressure Systems and Safety (MOE), School of Mechanical and Power Engineering, East China University of Science and Technology, Shanghai 200237, PR China

<sup>b</sup> Shanghai Engineering Research Center of Power Generation Environment Protection, Shanghai University of Electric Power, Shanghai 200090, PR China

<sup>c</sup> School of Electronic and Electrical Engineering, Sungkyunkwan University, Gyeonggi 440-746, Republic of Korea

## HIGHLIGHTS

- Solid solar cells based on FeS<sub>2</sub> or PbS NCs showed power conversion efficiency (PCE) of 3.0% and 3.11%, respectively.
- The FeS<sub>2</sub> NCs/polymer solar cells showed good time and thermal stability when exposed in air condition.
- Ternary solid solar cells based on PbS NCs exhibited a higher short circuit current density ( $J_{sc}$ ).

## ARTICLE INFO

### Article history:

Received 4 August 2015

Received in revised form 21 March 2016

Accepted 10 April 2016

Available online 23 April 2016

### Keywords:

FeS<sub>2</sub> nanocrystals

Polymer

Solid solar cell

Photovoltaic conversion efficiency

Stability

## ABSTRACT

Nanocrystal/polymer solid solar cells have the advantages of low-cost, simple process, and flexible manufacture. In this work, ternary solid solar cells based on FeS<sub>2</sub> and PbS nanocrystals exhibited photovoltaic conversion efficiency of 3.0% and 3.1%, respectively. As a kind of semiconductor with optical absorption in the visible and near-infrared regions, FeS<sub>2</sub> nanocrystals matched well with the solar radiation spectrum. Furthermore, PbS Nanocrystals could increase the number of electrons, due to its multiple exciton effect. Additionally, the FeS<sub>2</sub> nanocrystals solar cells showed high stability, with 83.3% of its initial efficiency remained after 15 weeks of exposure in air, and kept good stable performance at 20–80 °C. The photovoltaic conversion efficiency fluctuation magnitudes were also found to be smaller than quantum-dot sensitized solar cell under the same conditions.

© 2016 Published by Elsevier Ltd.

## 1. Introduction

Renewable energy is regarded as an essential supplement to the fossil fuels. Among the various renewable energy resources such as solar energy, wind energy, geothermal energy, biological energy, hydropower, hydrogen energy and wave energy [1], solar energy with the excellent advantages of abundance and non-polluting nature is supposed to be a great potential candidate [2]. Exploitation of solar energy is aimed to convert sunlight/solar radiation into electricity via photovoltaic devices like solar cells. In 1954, Yamaguchi et al. [3] successfully invented a silicon solar cell with a photovoltaic conversion efficiency (PCE) of 6%, which was regarded as the first generation of solar cells. The second generation of solar cell, the copper indium gallium selenium (CuInGaSe) thin film solar cell, which was developed in early 1989 with its PCE reached up to 13% [4]. However, the further development of these two generation

solar cells were restricted owing to the high cost of pure silicon and pollution issues. In recent years, Ito et al. [5] reported a bifacial dye-sensitized solar cell structure with a porous TiO<sub>2</sub> layer that provided high photo-energy conversion efficiency. Near infrared absorption of CdSe<sub>x</sub>Te<sub>1-x</sub> alloyed quantum dot [6] was used to prepare the quantum dot-sensitized solar cells (QDSSCs). Polymer solar cells based on P3HT, porphyrin-modified ZnO nanorods [7] and self-assembled monolayers [8] have been extensively investigated. Nevertheless, DSSCs and QDSSCs show poor stability since their liquid electrolyte leaks, and polymer solar cells with low efficiency for the slow electron transmission. Solid cells combined semiconductor NCs and polymers are one of the most promising alternatives to conventional silicon solar cells.

In the system of NCs/polymer solid solar cells, both the semiconductor NCs and the polymers were served as sunlight absorbers and exciton generators as well as electron donor. Electron transmission was much faster in NCs than that in polymers. By tuning the size, composition and shape of NCs, the absorption wavelength could be matched with the solar radiation spectrum. Moreover,

\* Corresponding author.

E-mail address: [luan@ecust.edu.cn](mailto:luan@ecust.edu.cn) (W. Luan).

## Nomenclature

### Abbreviation

PCE	photovoltaic conversion efficiency
NC	nanocrystal
DSSC	dye-sensitized solar cell
QDSSC	quantum dot-sensitized solar cell
FF	fill factor
LUMO	lowest unoccupied molecular orbital
P3HT	poly (3-hexylthiophene-2,5-diyl)
PCBM	[6,6]-phenyl C61 butyric acid methyl ester
PEDOT:PSS	poly(3,4-ethylenedioxythiophene)-poly(styrenesulfonate)
PbS	lead (II) sulfide
FeS <sub>2</sub>	ferrous disulfide

### Symbols

$V_{oc}$	open voltage
$J_{sc}$	short circuit current density
$J-V$	current density versus voltage
$P_{in}$	incident irradiation intensity
$M_n$	molecular weight

### Greek symbol

$\alpha$	photovoltaic conversion efficiency fluctuations coefficient
$\eta$	photovoltaic conversion efficiency

polymer materials like P3HT have achieved great progress in stability and overcome the disadvantages of materials such as polyurethane benzene phosphite vinyl (PPV), whose branching chains are prone to oxidatively decompose under illumination. Solid thin solar cells were prepared with materials like P3HT-capped CdSe superstructures [9], which could enhance the light harvest ability of active layer. TiO<sub>2</sub> NCs as photoelectrode was modified by metal-free organic dye [10]. Thus, combining the strengths of NCs and polymers showed great potential for achieving high efficiency and stability.

In the past five years, Yuan et al. [11] have conducted lots of research on the fabrication of pure and high-quality FeS<sub>2</sub> NCs for solar cells via facile solvothermal and hydrothermal reaction processes. Compared with the typical CdSe, CdTe, and CdS NCs materials, FeS<sub>2</sub> NCs were not only nontoxic, but also of low band gap (about 1.0 eV) and cost performance. Somnath et al. [12] reported inorganic solar cell based on ITO/PEDOT:PSS/MEH-PPV:FeS<sub>2</sub>/Al structure, which had the PCE of 0.064% and  $V_{oc}$  of 0.72 V. Bi et al. [13] used a kind of FeS<sub>2</sub> NCs to improve the stability and photo response in an ITO/FeS<sub>2</sub> NCs/Al device. Lin et al. [14] enhanced solar cell performance by adding FeS<sub>2</sub> NCs into P3HT:PCBM and a PCE of 2.3% was achieved. Because of the low band gap, variable sizes and shapes of PbS NCs, which showed potentially applicable in solar cells [15].

In this study, the ternary inverted bulk heterojunction solar cells with structure: FTO/TiO<sub>2</sub>/P3HT:PCBM:NCs/PEDOT:PSS/Ag were fabricated. The performance of devices was measured with a Keithley 2400 source measurement unit and a solar simulator. PbS and FeS<sub>2</sub> NCs were used to add into the active layer with different concentration, respectively. TiO<sub>2</sub> and PEDOT:PSS layer were introduced to act as the electron selective layer and hole selective layer, respectively. The results showed that FeS<sub>2</sub> NCs and PbS NCs in active layer could enhance the performance of devices, and a high efficiency of 3.11% and 3.0% were achieved, respectively. The FeS<sub>2</sub> ternary solar cell showed high stability in long-term and high temperature environment, and PCE fluctuations of FeS<sub>2</sub> NCs/polymer solar cell were smaller than QDSSCs under different irradiation intensities. These results indicated that the moderate NCs could improve the performance of inverted bulk heterojunction solid solar cells by improving the conductivity of the device.

## 2. Experimental

### 2.1. Materials and preparation of FeS<sub>2</sub> and PbS NCs

[6,6]-Phenyl C61-butyl acid methyl ester (PCBM) (99.5%) was purchased from Nano-C, USA. Two kinds of molecular weight

(15,000–45,000, and 54,000–75,000) of regioregular poly (3-hexylthiophene-2,5-diyl) (P3HT) (90%) were purchased from Sigma Aldrich, USA. Poly (3,4-ethylenedioxythiophene)-poly (styrenesulfonate) (PEDOT:PSS) was purchased from Sigma Aldrich. All materials were used as received without any further purification. FeS<sub>2</sub> NCs were synthesized via a solvothermal reaction process which was similar with the literature [11]. The as-prepared FeS<sub>2</sub> NCs were dispersed in chloroform and washed with excess acetone to remove organic impurities before using. High-quality PbS NCs was synthesized by the aqueous synthesis method [15], then dispersed in acetone, and washed with excess ethanol before using.

### 2.2. Active layer solution preparation

The active polymer solution was prepared by dissolving 40 mg P3HT and 40 mg PCBM in 2 mL chlorobenzene. Subsequently, a certain amount of FeS<sub>2</sub> or PbS NCs was added to prepare active layers solutions with different concentrations. The high and small  $M_n$  of P3HT were used to prepare PbS NCs and FeS<sub>2</sub> NCs/polymer solar cells, respectively. The hybrid solutions were treated with ultrasonication for more than 1 h to ensure that the NCs were uniformly dispersed, and the hybrid solution was placed for 24 h at room temperature.

### 2.3. Experimental setup and device fabrication

The NCs/polymer solar cells were prepared with an inverted structure, which was shown in Fig. 1. Where TiO<sub>2</sub> and PEDOT:PSS acted as the electron selective layer and hole selective layer, respectively. The preparation of NCs/polymer solar cells processes were shown in Fig. 2, firstly, the glass substrate pre-coated with

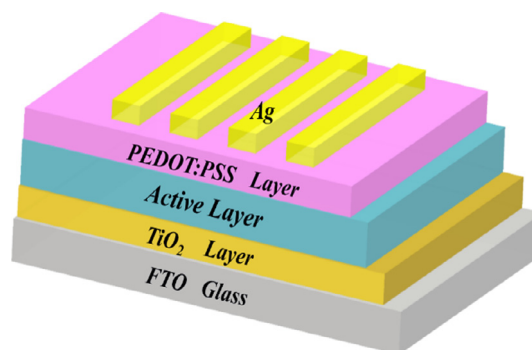


Fig. 1. Schematic architecture of the hybrid inverted solar cell.

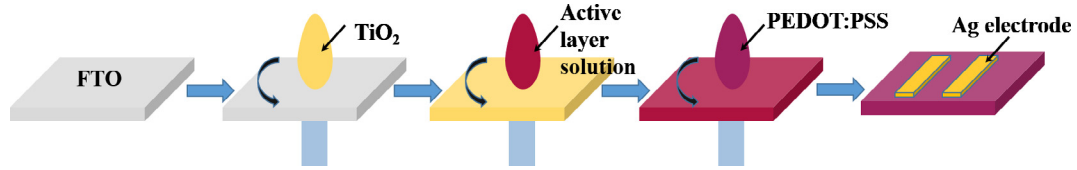


Fig. 2. Schematic diagram of the hybrid inverted solar cell preparation process.

fluorine tin oxide (FTO) (with size of 2 cm × 2 cm, 15 Ω/square) was cleaned in an ultrasonic bath with deionized water, acetone and isopropyl alcohol for 15 min, respectively. Then it was dried in a drying oven. Secondly, TiO<sub>2</sub> solution was spin-coated with 5000 rpm onto the FTO substrate, and sintered at 500 °C for 1 h. Thirdly, the active layer solution was spin-coated on the top of TiO<sub>2</sub> layer, and the blend films were placed on a hot plate and annealed at the temperature of 150 °C for 15 min. Subsequently, the PEDOT:PSS layer was spin-coated on the active layer and annealed at 160 °C for 5 min. Finally the Ag electrode was prepared by thermal evaporation as the counter electrode with an active area of 0.1 cm<sup>2</sup>.

2.4. Characterization

The current density versus voltage (*J*–*V*) characteristic of the solar cells was measured with a Keithley 2400 source measurement unit and a solar simulator (Abet Technologies, USA) under AM 1.5 (1000 W/m<sup>2</sup>) irradiation. The power conversion efficiency of solar cells could be calculated by Eq. (1), where *V*<sub>oc</sub>, *J*<sub>sc</sub>, *FF*, *P*<sub>in</sub> are open voltage, short current density, fill factor and the incident irradiation intensity, respectively. The time stability of the solar cell was evaluated by continuous *J*–*V* measurement for 15 weeks. The thermal stability of the solar cells was investigated by putting devices in different temperature from 20 to 80 °C and the *J*–*V* characteristic was recorded. Additionally, the magnitudes of PCE fluctuation in a different irradiation intensity from 200 W/m<sup>2</sup> to 1500 W/m<sup>2</sup> were calculated. Surface morphology of active layer films were characterized by using atomic force microscope (AFM, Veeco) in non-contact mode.

$$\eta = \frac{V_{oc} J_{sc} FF}{P_{in}} \times 100\% \tag{1}$$

3. Results and discussion

3.1. The effects of FeS<sub>2</sub> and PbS NCs in the solid solar cell

The *J*–*V* characteristics of solar cells which were prepared with different concentrations of FeS<sub>2</sub> are showed in Fig. 3(a). The open

voltages (*V*<sub>oc</sub>) of all the prepared devices were held around 0.6 V. Moreover, obvious enhancement in short circuit current density (*J*<sub>sc</sub>) was observed at the FeS<sub>2</sub> concentration of 1.25 mg/mL. In comparison, the best PbS NC cell exhibited a short circuit current density (*J*<sub>sc</sub>) of 16.03 mA/cm<sup>2</sup>, an open circuit voltage (*V*<sub>oc</sub>) of 0.56 V, and a fill factor (*FF*) of 34.63%. The efficiency of 3.11% was obtained at a PbS NC concentration of 2.4 mg/mL. Fig. 3(b) shows the *J*–*V* characteristics of PbS solar cells with different PbS NC concentrations.

The performance of solar cells with different concentrations of high quality FeS<sub>2</sub> NCs are listed in Table 1. According to the results, the addition of FeS<sub>2</sub> NCs from 0 to 1.25 mg/mL increased the *J*<sub>sc</sub> from 8.84 to 10.11 mA/cm<sup>2</sup>, which resulted in the improvement of the PCE from 2.8% to 3.0%. The performance of device was higher than the literature reported [14]. This was attributed to the improved light harvesting capability of the FeS<sub>2</sub> NCs in the solar

Table 1 Photovoltaic parameters of solid solar cells fabricated with different concentrations of FeS<sub>2</sub> NCs.

Concentration (mg/mL)	<i>J</i> <sub>sc</sub> (mA/cm <sup>2</sup> )	<i>V</i> <sub>oc</sub> (V)	<i>FF</i> (%)	PCE (%)
0	8.84	0.61	51.9	2.8
1.25	10.11	0.60	50.2	3.0
2.5	9.12	0.59	47.6	2.6
3.75	8.51	0.59	48.5	2.4
5	8.10	0.58	44.3	2.1
6.25	7.91	0.58	40.7	1.9
7.5	7.84	0.59	41.5	1.9

Table 2 Photovoltaic parameters of solid solar cells fabricated with different concentrations of PbS NCs.

Concentration (mg/mL)	<i>J</i> <sub>sc</sub> (mA/cm <sup>2</sup> )	<i>V</i> <sub>oc</sub> (V)	<i>FF</i> (%)	PCE (%)
0	16.17	0.553	33.91	3.03
0.975	15.53	0.565	33.76	2.97
1.6	14.56	0.566	34.32	2.83
2	14.67	0.563	34.94	2.89
2.4	16.03	0.560	34.63	3.11
3	13.50	0.565	34.62	2.64
3.5	16.38	0.562	32.48	2.99

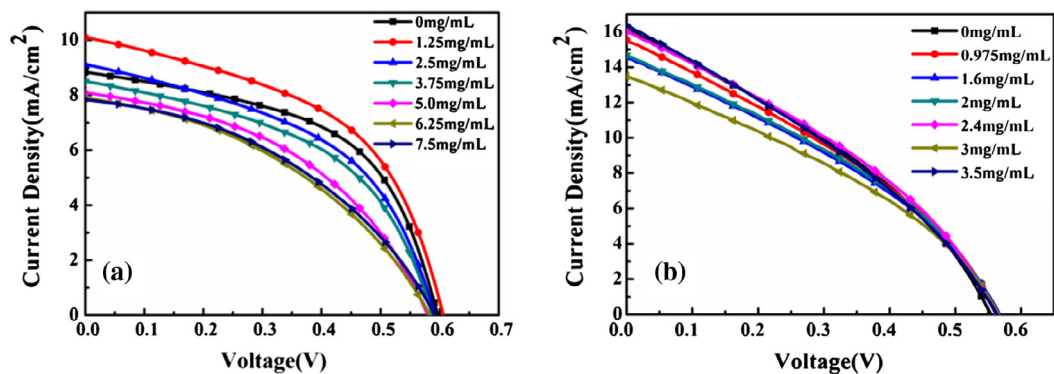
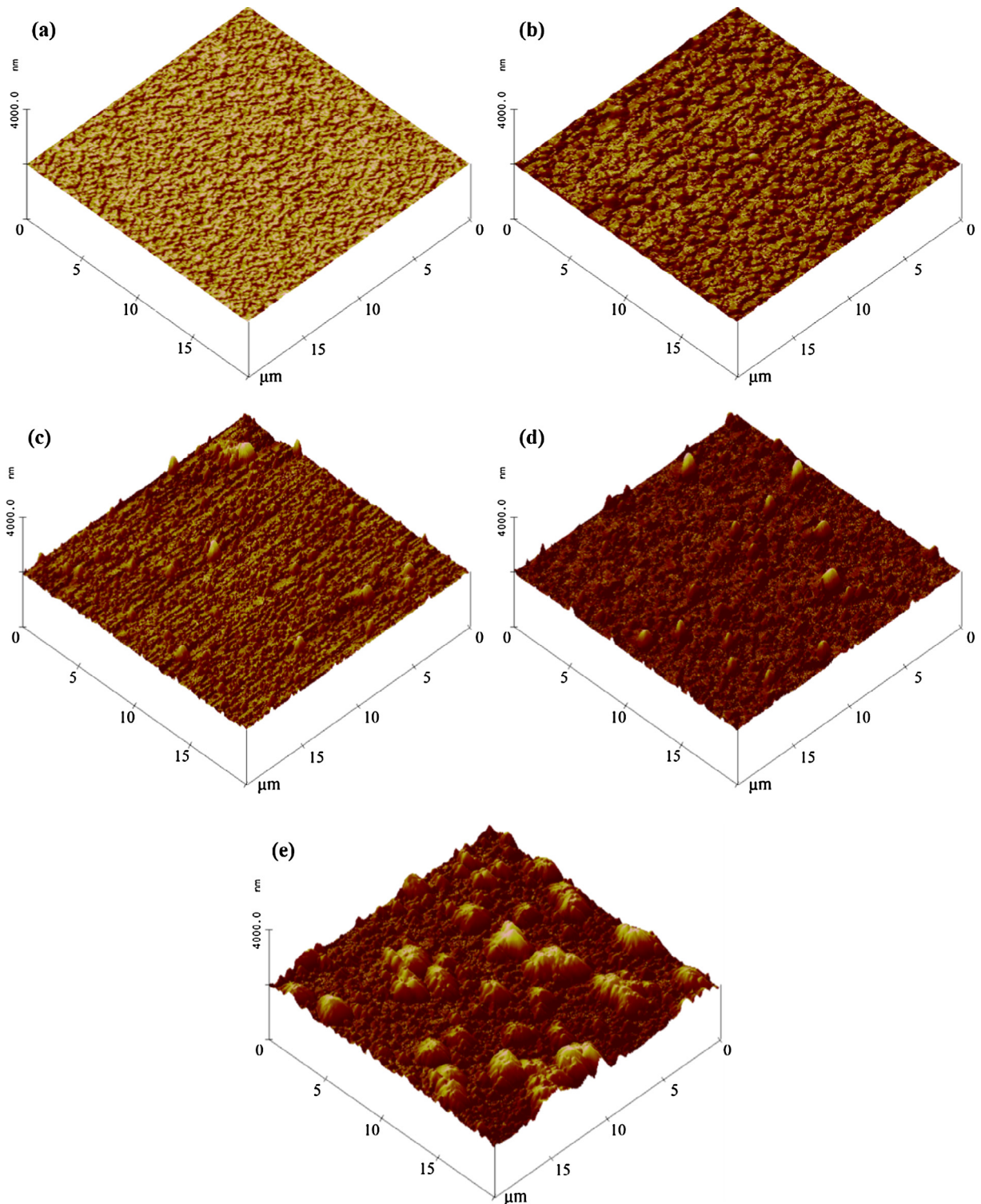


Fig. 3. *J*–*V* characteristics of fabricated solar cells containing different concentrations of (a) FeS<sub>2</sub> NCs, (b) PbS NCs.

cell. However, when the NCs concentration was further increased from 2.5 mg/mL to 7.5 mg/mL, the  $J_{sc}$  showed a decreasing trend, and the fill factor ( $FF$ ) and the PCE also went down.

The devices performance with different concentrations of high quality PbS NCs are listed in Table 2. Compared with  $FeS_2$ -based solar cells, the PbS NCs/polymer solar cells possessed relatively higher  $J_{sc}$ , PCE and lower  $FF$  values. The  $V_{oc}$  values of both two kinds of solar cells were basically flat. With the introduction of low

concentration (0.975 mg/mL) of PbS NCs, a decreased PCE was found. It was because the nanocrystal surface defect effect was greater than the multiple exciton effects [16]. With the increase of the concentration, the multiple exciton effects gradually dominated the performance of device. However, too much PbS NCs addition would influence the performance of film, accordingly, the PCE of the PbS NCs/polymer solar cells firstly increased and then declined. The best PCE of 3.11% was obtained at a PbS NCs concen-



**Fig. 4.** AFM image of P3HT:PCBM thin films with different addition amount of  $FeS_2$  NCs (a) 0 mg/mL, (b) 1.25 mg/mL, (c) 2.5 mg/mL, (d) 3.75 mg/mL.



tration of 2.4 mg/mL. Comparing with the non-PbS NCs organic solar cell, the power conversion efficiency of the cells with PbS NCs was improved.

In order to further analyze the effect of FeS<sub>2</sub> NCs, AFM was used to observe the evolution of morphology of P3HT:PCBM:FeS<sub>2</sub> thin

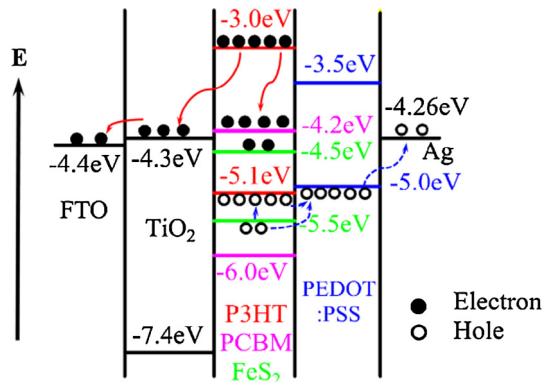


Fig. 5. Schematic diagram of the energy levels in the FeS<sub>2</sub> NCs/polymer solar cells.

**Table 3**  
Photovoltaic parameters of FeS<sub>2</sub> NC/polymer solar cell after different operating time.

Duration time (week)	J <sub>sc</sub> (mA/cm <sup>2</sup> )	V <sub>oc</sub> (V)	FF (%)	PCE (%)
0	10.11	0.60	50.2	3.0
1	9.66	0.60	50.3	2.9
2	9.28	0.59	48.8	2.7
3	8.84	0.60	53.1	2.8
5	8.71	0.60	52.4	2.7
7	8.56	0.59	52.5	2.7
10	8.45	0.59	52.5	2.6
15	8.19	0.60	50.6	2.5

films. Blend films with different addition amount of FeS<sub>2</sub> NCs were placed on a hot plate and annealed at the temperature of 150 °C for 15 min, after annealing treatment, the blend films not only removed excess organic solvent to increase the degree of phase separation, but also decreased the roughness of the film, the corresponding results are presented in Fig. 4. The AFM images show the 3-D topography and the roughness of active layer films. The r.m.s roughness of 0 mg/mL film was 5.338 nm, and the r.m.s roughness of 1.25 mg/mL film, 2.5 mg/mL film, 3.75 mg/mL and 5 mg/mL film were 14.120 nm, 50.068 nm, 70.157 nm, and 165.510 nm, respectively. The texture of 0 mg/mL film was much smoother than other films. However, the best device was obtained with a small amount of 1.25 mg/mL NC added into the active layer, the r.m.s roughness of film increased a little. Due to the low extent of surface roughness increase, the charge transport distance would effectively reduce and the internal reflection of light and light absorption would dramatically enhance. Thus, the short current density and the performance of device had also increased [17]. When more NCs added, the performance of the blend films would degraded, which was due to the defects in thin film increased and the charge was captured rather than to the corresponding electrode. The results indicated that a certain amount of NCs could help to increase the efficiency of the device.

In the irradiation condition, both the polymer P3HT and FeS<sub>2</sub> NCs could generate excitons. The excitons separated into electrons and holes at the donor–acceptor interfaces. As shown in Fig. 5, electrons were able to transfer from P3HT to TiO<sub>2</sub> and PCBM. Because the LUMO of FeS<sub>2</sub> (−4.5 eV) was lower than that of TiO<sub>2</sub> (−4.3 eV), the electrons generated by FeS<sub>2</sub> NCs could not reach TiO<sub>2</sub> layer, which resulted in a lower efficiency of electron collection. Holes transportation functioned inversely, the holes were generated by the FeS<sub>2</sub> NCs could be transferred to PEDOT:PSS and P3HT, which means that many more holes could be converted into photocurrent. When the solid solar cell contained fewer FeS<sub>2</sub>

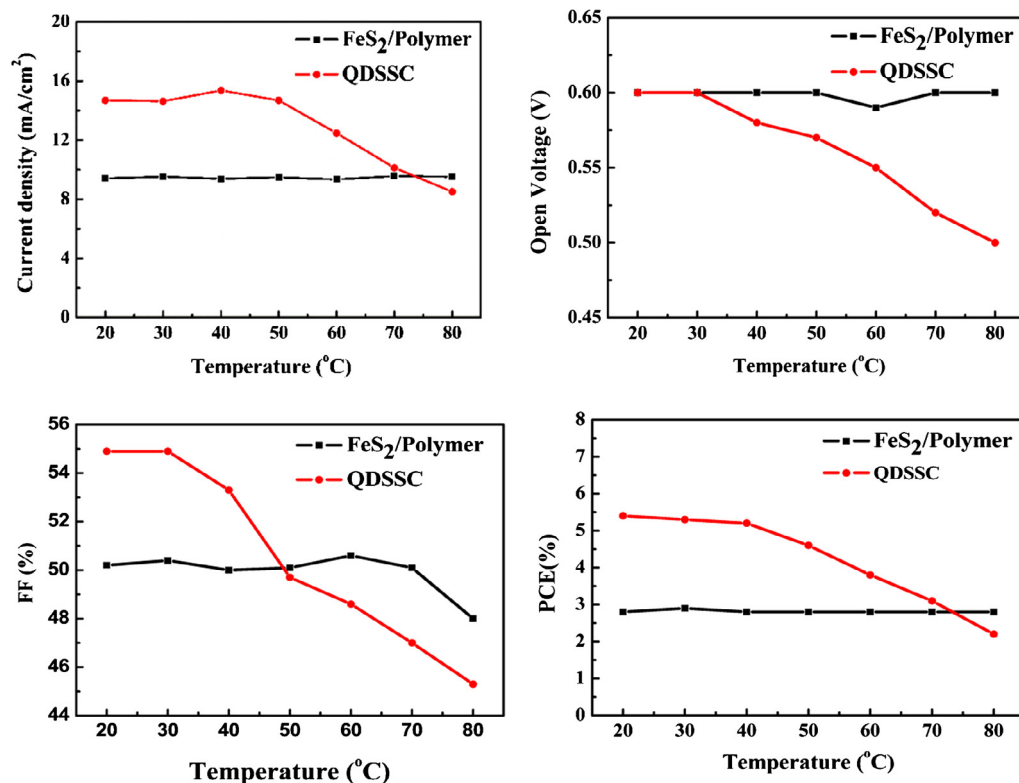


Fig. 6. Thermal stability comparison of FeS<sub>2</sub> NC/polymer solar cell and QDSSC.

NCs (i.e., 1.25 mg/mL), the FeS<sub>2</sub> NCs advantages of near-infrared absorption and rapid transmission of carriers were greater than its deficiency in electronic transmission. Therefore, the FeS<sub>2</sub> NCs/polymer solar cell displayed better performance than the polymer solar cell. When the concentration of FeS<sub>2</sub> NCs in the solar cell was higher, its deficiency was more dominant than its advantages, resulting in a large number of electrons unable to transfer. Thus,  $J_{sc}$  decreased gradually, which would also cause the PCE to decline. This is the reason why the present solid solar cells based on FeS<sub>2</sub> NCs exhibited the optimized efficiency at a certain concentration of FeS<sub>2</sub>.

### 3.2. Time and thermal stabilities of FeS<sub>2</sub> NC/polymer solar cell

Although there are many reports on the high PCE of QDSSCs, the liquid electrolyte systems of QDSSCs used to have a common and severe problem of leakage that lead to a short working life. The time stability and thermal stability of the NCs/polymer solar cell with a FeS<sub>2</sub> NCs concentration of 1.25 mg/mL were investigated. The solar cells were stored in a petri dish at the ambient temperature without further seal. The results are summarized in Table 3. During the measurement period of 15 weeks, the  $J_{sc}$  of the cell decreased gradually from 10.11 mA/cm<sup>2</sup> to 8.19 mA/cm<sup>2</sup>. The PCE declined from 3.0% to 2.5%. That means 83.3% of the original efficiency of the cell remained after 15 weeks. Compared with other literatures [12,18], the FeS<sub>2</sub> NCs solid solar cells exhibited higher time stability.

The thermal stability of the cell in the range of 20–80 °C is illustrated in Fig. 6. Fig. 6 showed that only the FF of FeS<sub>2</sub> NCs/polymer solar cell slightly decreased when the temperature raised from 70 °C to 80 °C. The  $J_{sc}$ ,  $V_{oc}$ , and PCE values of the FeS<sub>2</sub> NCs/polymer solar cell almost remained the same at every temperature, while those of the QDSSCs showed a sharp decline with increasing temperature. Because of its liquid electrolyte, the QDSSCs was more suitable for operation between 20 and 40 °C. While the FeS<sub>2</sub> NCs/polymer solar cell displayed a wider working temperature range from 20 °C to 80 °C and an excellent stability.

### 3.3. PCE fluctuation of fabricated solar cells under different irradiation intensity

Irradiation intensity is not constant during the daytime. Generally, the standard irradiation intensity was 1000 W/m<sup>2</sup>, which was corresponded to the standard PCE ( $\eta_{1000}$ ) value of 2.4% in this paper. The influence of irradiation intensity changing from 200 W/m<sup>2</sup> to 1500 W/m<sup>2</sup> was investigated. The device could absorb more light and generate more excitons with increasing light intensity. It is the reason why the PCE was found to be proportional to the light intensity (as shown in Table 4). The prepared solar cell of PCE fluctuations coefficient ( $\alpha$ ) was calculated and the fluctuation coefficient ( $\alpha$ ) was described as Eq. (2). Comparing with that

of the QDSSCs, the PCE fluctuation magnitudes of the QDSSCs were always larger than those of the FeS<sub>2</sub> NCs/polymer solar cell at different irradiation intensity.

$$\alpha = \frac{\eta - \eta_{1000}}{\eta_{1000}} \times 100\% \quad (2)$$

In summary, the NCs/polymer solar cells showed better photovoltaic conversion efficiency, which was affected slightly by irradiation intensity, and almost had no influence with temperature. Meanwhile, the substrate FTO glass can be replaced by flexible substrate, and it makes the solar cell a flexibility characteristic. Thus, the solar cells can be used in the solar backpack, solar cars, building integrated photovoltaic (BIPV) and so on. Due to these characteristics, the solar cells can inherit in the windows, roof, and wall or inside the wall.

Photovoltaic cells based on polymer and inorganic nanoparticles bulk heterojunction composites, which have the potential for renewable energy resources. It is because not only their lightness, low cost and simple fabrication processing in large area, but also the electron transport in nanoparticles is indeed faster than the electron mobility in polymers. The inorganic nanoparticles usually have higher holes transport properties, at the same time, it can also improve the light absorption in the active layer due to the specific advantage for light harvesting. Hybrid solar cells based organic/inorganic has gained a lot of attention in market of solar cells, but there still have many problem to solve, such as low efficiency, suitable material, and inorganic nanoparticles this area still needs to be explored deeply.

## 4. Conclusion

FeS<sub>2</sub> or PbS NCs based solid solar cells were prepared with an inverted structure. The addition of NCs into polymer solar cells resulted in an enhanced light harvesting ability and a correspondingly obvious increased in  $J_{sc}$ . High loading of FeS<sub>2</sub> NCs or PbS NCs were found to reduce electron transmission ability. The solid solar cell exhibited an optimal PCE of 3.0% at a FeS<sub>2</sub> NC concentration of 1.25 mg/mL, and a PCE of 3.0% with a PbS NCs concentration of 2.4 mg/mL. The optimized FeS<sub>2</sub> NCs-based solar cell kept high stability 83.3% of its initial efficiency after exposing in air for 15 weeks. And the device exhibited good stable performance between 20 °C and 80 °C. Furthermore, the PCE fluctuation magnitudes of the cells showed better than those of a QDSSC under the same conditions.

## Acknowledgements

The authors gratefully acknowledge financial support from the National Natural Science Foundation of China (51172072, 51475166).

## References

- [1] Mathiesen BV, Lund H, Connolly D, Wenzel H, Østergaard PA, Möller B, et al. Smart energy systems for coherent 100% renewable energy and transport solutions. *Appl Energy* 2015;145:139–54.
- [2] Luthander R, Widén J, Nilsson D, Palm J. Photovoltaic self-consumption in buildings: a review. *Appl Energy* 2015;142:80–94.
- [3] Yamaguchi M, Ohshita Y, Arafune K. Present status and future of crystalline silicon solar cells in Japan. *Sol Energy* 2006;80:104–10.
- [4] Chirila A, Blosch P, Pianezzi F. Potassium-induced surface modification of Cu (In, Ga)Se<sub>2</sub> thin films for high-efficiency solar cells. *Nat Mater* 2013;12:1107–11.
- [5] Ito S, Zakeeruddin SM, Comte P. Bifacial dye-sensitized solar cells based on an ionic liquid electrolyte. *Nature Photon* 2008;2:693–8.
- [6] Pan ZX, Zhao K, Zhong XH. Near infrared absorption of CdSe<sub>x</sub>Te<sub>1-x</sub> alloyed quantum dot sensitized solar cells with more than 6% efficiency and high stability. *J Am Chem Soc* 2013;7:5215–22.

**Table 4**

Comparison between PCE fluctuation magnitudes of FeS<sub>2</sub> NC/polymer solar cell and QDSSCs.

Intensity (W/m <sup>2</sup> )	FeS <sub>2</sub> NC/polymer solar cell		QDSSCs	
	PCE (%)	$\alpha$ (%)	PCE (%)	$\alpha$ (%)
200	1.0	−58.3	1.8	−66.0
350	1.5	−37.5	3.1	−41.5
500	1.9	−20.8	4.1	−22.6
800	2.2	−8.3	4.8	−9.4
1000	2.4	0.0	5.3	0.0
1200	2.5	4.2	5.8	9.4
1500	2.7	12.5	6.3	18.9

- [7] Said AJ, Poize G, Martini C. Hybrid bulk heterojunction solar cells based on P3HT and porphyrin-modified ZnO nanorods. *J Phys Chem C* 2010;114:11273–8.
- [8] Chiu JM, Chu CC, Zena DM, Tai Y. Simultaneous enhancement of photocurrent and open circuit voltage in a ZnO based organic solar cell by mixed self-assembled monolayers. *Appl Energy* 2015;160:681–6.
- [9] Peng YL, Song GH, Hu XH, He GJ, Chen ZG, Xu XF, et al. In situ synthesis of P3HT-capped CdSe superstructures and their application in solar cells. *Nanoscale Res Lett* 2013;8:106–13.
- [10] Zhang W, Zhu R, Liu B, Ramakrishna S. High-performance hybrid solar cells employing metal-free organic dye modified TiO<sub>2</sub> as photoelectrode. *Appl Energy* 2012;90:305–8.
- [11] Yuan B, Luan W, Tu S. One-step synthesis of cubic FeS<sub>2</sub> and flower-like FeSe<sub>2</sub> particles by a solvothermal reduction process. *Dalton Trans* 2012;41:772–6.
- [12] Somnath M, Animesh L, Arka D, Partha PR. Synthesis of nanocrystalline FeS<sub>2</sub> with increased band gap for solar energy harvesting. *J Mater Sci Technol* 2014;30(8):770–5.
- [13] Bi Y, Yuan YB, Exstrom CL, Darveau SA, Huang JS. Air stable photo-sensitive, phase pure iron pyrite nanocrystal thin films for photovoltaic application. *Nano Lett* 2011;11:4953–7.
- [14] Lin CW, Wangb DY, Wangb YT, Chen CC, Yang YJ, Chen YF. Increased photocurrent in bulk-heterojunction solar cells mediated by FeS<sub>2</sub> nanocrystals. *Sol Energy Mater Sol Cells* 2011;95:1107–10.
- [15] Anil K, Anshuman J. Photophysics and charge dynamics of Q-PbS based mixed ZnS/PbS and PbS/ZnS semiconductor nanoparticles. *J Colloid Interf Sci* 2006;297:607–17.
- [16] Warner J, Cao H. Shape control of PbS nanocrystals using multiple surfactants. *Nanotechnology* 2008;19:305605–9.
- [17] Huang YC, Liao YU, Li SS, Wu MC, Chen CW, Su WF. Study of effect of annealing process on the performance of P3HT/PCBM photovoltaic devices using scanning-probe microscopy. *Sol Energy Mater Sol Cells* 2009;93:888–92.
- [18] Richardson BJ, Zhu L, Yu QM. Inverted hybrid solar cells based on pyrite FeS<sub>2</sub> nanocrystals in P3HT:PCBM with enhanced photocurrent and air-stability. *Sol Energy Mater Sol Cells* 2013;116:252–61.